Three-Dimensional Dynamic Response Model for Rigid Pavements

JAGANNATH MALLELA AND K. P. GEORGE

Traditionally, elastic layer analysis has been employed in pavement design and evaluation. Three basic assumption of elastic layer analysis are that static loading, linear elastic materials, and infinite areal extents of layers are each inconsistent with real-world pavement structure. In an effort to resolve the issue, finite element techniques were used in this research. The three-dimensional finite element program ABAQUS (3D-DFEM) was employed to analyze pavements subjected to dynamic loading. Preliminary studies included a sensitivity analysis to formalize various aspects of the finite element model (e.g., mesh size and boundary conditions). Studies were conducted with 3D-DFEM to verify its static and dynamic analysis capabilities. Static results compared favorably with those in a previous study. The 3D-DFEM responses of an in-service flexible pavement were in agreement with measured falling-weight deflectometer (FWD) deflections and those predicted by an elastodynamic solution. Having verified both those capabilities, the model was employed for calculating deflection responses of factorially designed rigid pavement structures. Thicknesses and moduli of pavement layers varied over a wide range. A 9,670-lb FWD load with seven deflection sensors was configured. Statistical equations, one for each sensor position, were derived employing the deflection data base assembled from the factorial experiment. These equations, in turn, were validated by predicting the measured responses of in-service rigid pavements. An important practical application of the equations is to improve the mechanistic interpretation of FWD data in backcalculation routines. The 3D-DFEM with its numerous features simulating real-world conditions eventually could replace elastic layer analysis.

During the past two decades, the emphasis in pavement engineering has been to maintain existing infrastructure through efficient and cost-effective management practices. Nondestructive testing of pavements, in conjunction with backcalculation techniques, has become a popular tool for in situ material characterization of pavements. Backcalculation can be thought of as the inverse process of obtaining material parameters of pavement layers from surface deflections under a given test load. Backcalculation depends on how well surface deflections can be predicted from pavement structure and material characteristics. For surface deflection calculation, layered elastic theory is the preeminent choice. However, as currently used, elastostatic analysis assumes static loading conditions, infinite layers in the lateral direction, and linear elastic materials—all simplifications of the real-world problem. For example, loading mode has a tremendous effect on pavement response. Mamlouk (*1*) compares the effect of steady-state loading mode with that of static loading mode and reports an error of 24 percent predicted through static analysis. Sebaaly et al. (*2*) report that static analysis of pavement response to the FWD load always results in average surface deflections 20 to 40 percent larger than field measurement. The effect of loading mode on pavement response cannot be overemphasized.

Department of Civil Engineering, University of Mississippi, University, Miss. 38677.

To improve upon the backcalculation procedures, Sebaaly et al. (*2*) suggest an elastodynamic approach using multiple degrees of freedom to predict dynamic response of pavements under FWD loading. Ashton and Moavenzadeh (*3*) present an analysis procedure for the determination of stresses and displacement in a three-layered viscoelastic system. These studies are aimed at resolving the issues of what effect loading mode and material characterization have and the major drawbacks of the layered theory approach. Although promising, those techniques are not widely applicable and lack the speed and simplicity of layered elastic models. Finite element techniques that are used extensively in the aerospace industry now are being applied to other engineering fields for which analytical solutions have not been readily available. Finite element codes used for rigid pavement analysis, FIDIES (*4*), H51ES (*5*), ILLISLAB (*6*), GEOSYS (*7*), are each tailored to solve a specific problem. Whether dynamic load is more appropriate for simulating truck and FWD loading in the field is still debated. With the advent of supercomputers, large, general purpose finite-element codes have been developed that take advantage of their speed and memory capabilities. ABAQUS (*8*), referred to as 3D-DFEM, is one such finite element code; it was developed mainly for structural analysis. The program is capable of modeling any wheel-gear combination, or static, steady-state dynamic, impulse, or user-defined loading. Pavement discontinuities, loss of support conditions, and a variety of material behavior also can be implemented in the program code, providing a versatile tool for pavement analysis. Zaghloul et al. (*9,10*) used the code to conduct flexible pavement analysis.

The purpose of this study is to explore the use of a three-dimensional dynamic finite element program (3D-DFEM) in rigid pavement analysis. With the objective of validating the program for use in pavement analysis, static analyses were carried out and compared with analytical and other finite element solutions of some credibility. In addition, dynamic responses of 3D-DFEM were compared with FWD load response in the field and other numerical solutions.

Primary factors that affect pavement response are moduli and thickness of pavement layers. A factorial experiment was designed to investigate the effect of these factors on rigid pavement response, formalizing a comprehensive data base. Regression analysis was performed on this data base, developing statistical models for predicting dynamic pavement response. The models were validated by comparing the predicted responses with those measured under FWD load in two Strategic Highway Research Program (SHRP), General Pavement Studies (GPS) sections.

FINITE ELEMENT MODELING USING 3D-DFEM

An explicit integration scheme of the 3D-DFEM generally is more suitable for impact- or impulse-load analyses than an implicit

scheme. Accordingly, the former scheme was used for this study. The procedure is based on the implementation of an explicit integration rule together with diagonal or "lumped" element mass matrices. Equations of motion are integrated using the explicit central difference integration rule. Creating a finite element mesh with appropriate boundary features is a prerequisite to solving a boundary value problem. A preliminary study investigating the sensitivity of mesh size and boundary conditions, among other factors, was undertaken before attempting to solve a rigid pavement problem. The following features were thoroughly investigated leading to the final mesh configuration and attendant boundaries:

- Vertical and lateral subgrade extents,
- Pavement-shoulder interface,
- Material characterization,
- Mesh fineness and element aspect ratio, and
- FWD loading.

Vertical and Lateral Subgrade Extents

When applying numerical analysis procedures, it is important to eliminate the effect of boundaries on the responses. With this objective in mind, several finite element runs were performed to determine the depth and lateral extent to which the subgrade should be modeled. Consideration of a 12.2-m (40-ft) deep subgrade resulted in negligible (of the order 10^{-10} in. and less) deflections at the bottom boundary. Simulating this, the 12.2-m (40-ft) bottom boundary was assumed to permit no movement of the nodes lying on that boundary ($U_x = 0$, $U_y = 0$, $U_z = 0$). To determine the effect of lateral subgrade extent on pavement response, the subgrade was modeled to a distance of 3, 6, and 9.1 m (10, 20, and 30 ft) beyond the pavement edge. At each of these three distances, three different boundary conditions were tested: free, roller, and fixed. Vertical deflections at the center of the load from the nine runs were then compared (Figure 1). The finding that the response is virtually unaffected by a boundary beyond 9.1 m (30 ft) from the load has led to the adoption of a roller-type lateral boundary ($U_x = 0$, $U_y = 0$, $U_z \neq 0$) at 9.1 m (30 ft) from the pavement edge. Three undoweled concrete slabs, each 6.1 m (20 ft) long, were modeled in the direction of traffic. Introduction of dowel bars requires substantial meshing, adding to the complexity of the problem. In order to focus on the specific objective of the study, dowel bars were not modeled.

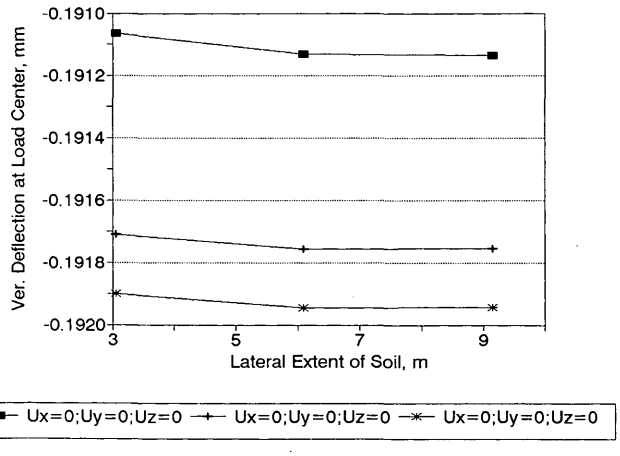

FIGURE 1 Effect of lateral soil extents and boundary conditions on deflection (1 mm = 39.37 mil; 1 m = 3.281 ft).

Pavement-Shoulder Interface

Because in the real world the proportion of concrete pavements having tied shoulders is relatively small, it was decided to model the pavement-shoulder interface as a discontinuity. That was accomplished by using special contact surface definitions provided in ABAQUS. In effect, the shoulder was not to provide any structural support to the pavement.

Material Characterization

Within the load range generally encountered in pavement design and analysis [standard 80-kN (18-kip) equivalent single axle load (ESAL)], stresses induced in each layer are not likely to exceed their respective elastic ranges. Elastic analysis is implemented accordingly.

Mesh Fineness and Element Aspect Ratio

One of the major precepts of finite element theory is to provide a finer mesh around areas of stress concentration than within the surrounding medium. Therefore, a fine uniform mesh with an element size of 75 mm (2.95 in.) was generated around the loaded area, and a nonuniform mesh with suitable "bias" factors was generated in the rest of the continuum. The biased mesh generation ensures a gradual change in the mesh size, with smaller elements in the vicinity and larger elements away from the load. Because three-dimensional linear elements were used, large elements away from the load helped to provide "quite" boundaries. The aspect ratio of the elements in the loaded area was kept below 2 for better precision. The surface layer was modeled as two sublayers (elements), the base and subbase were each modeled as a single element, and the subgrade was partitioned into five elements. By taking advantage of the symmetry afforded by the load placement, one-half or one-quarter of the problem was solved.

FWD Loading

Except for the static load comparison, for which an F-15 single wheel load was used, FWD loading was used for all other analyses. An FWD can simulate various load magnitudes; a peak load of 43 kN (9,670 lb) was adopted in this study. A finite element idealization of a typical load history (*11*) is presented in Figure 2, which indicates that the loading duration is about 25 msec. At 638 kPa (92.61 psi) contact pressure, the loaded area, assumed circular, is calculated to be 705 cm^2 (109.35 $in.^2$). The distributed circular loaded area is approximated using 12 square elements, each having a side length of 75 mm (2.95 in.). The 43-kN (9,670-lb) load is centered at the midsection of the slab, 3 ft from the edge of the pavement. Nodes are defined at various distances to match the location of the geophones measuring surface deflections for the FWD test. Figure 3 represents the final mesh configuration.

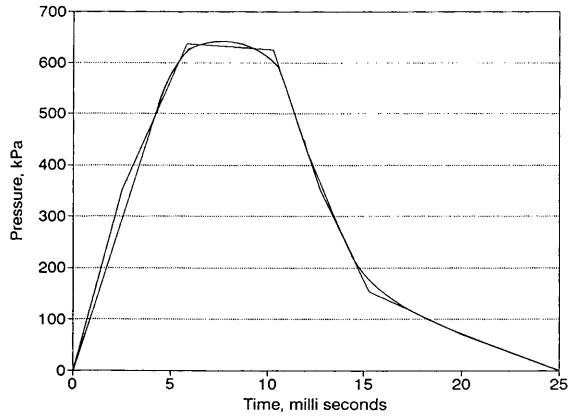

FIGURE 2 FWD load pulse simulated in the 3D-DFEM analysis (1 kPa = 0.145 psi).

As suggested by one of the reviewers, the authors have used the SHRP-FWD load pulse in the analysis (personal communication, Cheryl Richter, LTPP Division, FHWA; unpublished data). The average increase in deflection response with this pulse in weak pavements was 6.5 percent.

FEASIBILITY STUDIES OF ABAQUS

Validation of Static Analysis

In order to validate the analysis procedure of the 3D-DFEM, the authors configured and solved Ioannides and Donnelly's (*7*) slab-on-grade problem, which involves a slab on soft subgrade. Closed-form solutions are drawn from Losberg (*12*) with BISAR (*13*) and ILLISLAB (*5,6*) providing the layer elastic solutions. A finite element solution using the GEOSYS model (Table 1) with slightly different slab thickness is included for want of a better three-dimensional model. A single wheel load of an F-15 aircraft with a tire pressure of 2446 kPa (355 psi) and a total load of 133 kN (30 kips) was placed centrally on a slab-on-grade system. All of the materials were characterized as linear elastic. The continuum was modeled using eight noded, isoparametric, three-dimensional brick elements. Because of the symmetry of the model, only one-quarter of the slab was modeled. Table 1 presents a comparison of various solutions along with other pertinent details. The ABAQUS solution shows good agreement with BISAR, ILLISLAB, and closed-form solutions.

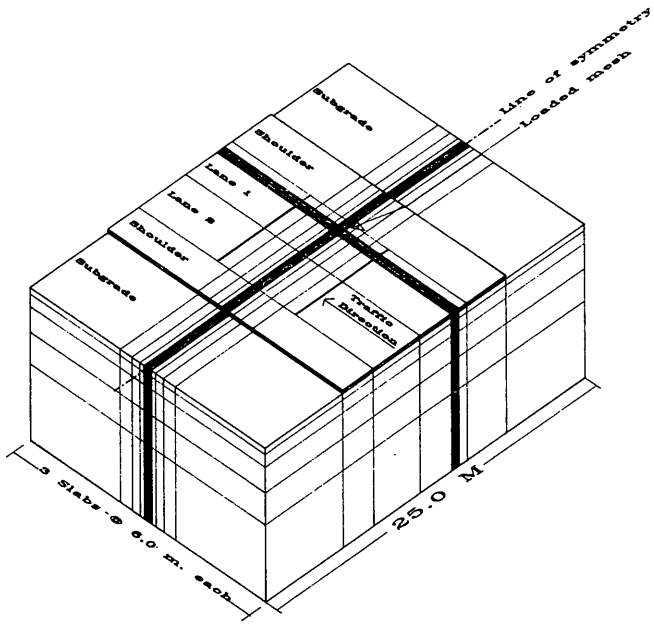

FIGURE 3 3D-DFEM problem showing partial mesh configuration (1 m = 3.281 ft).

Validation of Dynamic Load (FWD) Analysis

To verify the validity of the 3D-DFEM results, a theoretical analysis was performed on a typical in-service flexible pavement section. The pavement section originally was studied by Hoffman and Thompson (*14*) and later by Sebaaly et al. (*2*). Material properties were determined in the laboratory (*14*), except Poisson's ratios, which were assumed. Table 2 gives the material and geometric properties. The 3D-DFEM results are compared with the reported FWD measurements and the elastodynamic solution using the multilayer computer program DYNAMIC (*2*). Also included in this comparison is a static deflection basin using the DYNAMIC program with zero frequency load (or equivalent static solution).

The FWD used in field testing and simulated in the 3D-DFEM has a 30-cm (12-in.) diameter base plate; an impulse load of 36 kN (8 kips) was produced with a load duration of approximately 40 msec. The center of the load is at midsection, a distance of 910 mm (3 ft) from the edge of the pavement. The distributed loaded area is approximated using 12 square elements with 75-mm (2.95-in.) sides.

Measured and computed deflections at four geophone locations are compared in Figure 4. The 3D-DFEM deflections are reasonably close to the measured deflections; deviations are 5, 2, 9, and 34 percentage points at geophone locations 1, 2, 3, and 4, respectively (measured responses). Similar validation studies conducted by Zaghloul et al. (*10*) conclude that ABAQUS is indeed a feasible tool with which to perform nonlinear dynamic analysis of flexible pavements. The relatively large discrepancy at the fourth sensor may be attributable to the noise effect of reflected waves from the boundary. A new release of the 3D-DFEM (Version 5.2) provides an "infinite element" for modeling boundary by choosing suitable damping constants to minimize the reflection of dilatational and sheer-wave energy back into the model.

The fact that the 3D-DFEM results and nonlinear elastodynamic responses are in agreement is another indication that, for routine modeling, elastic characterization is adequate unless the pavement materials are extremely soft.

As pointed out in previously (*2*) and confirmed in this study, static analysis (as with BISAR) yields average deflection values approximately 25 to 30 percent higher than those obtained with 3D-DFEM on elastodynamic analysis.

TABLE 1 Comparison of Static Analysis Results (All Responses Measured at Center of Load)

RESPONSE	POSITION	ANALYSIS MODEL				
		Closed-form	ABAQUS-3D	BISAR	ILLISLAB-2D	GEOSYS*-3D
Vertical Deflection (mm)	Top of slab @ load center	1.07	1.04	1.02	1.04	0.82
Vertical stress (kPa)	Top of subgrade under the load	-45.6	-40.9	-44.9	-42.4	-34.7
Maximum bending Stress (kPa)	Bottom of slab under the load	5230	5121	5216	5483	4200

*The results from the GEOSYS model were based on a slab 203mm (8 inches) thick, whereas, the results from other models were based on a slab 183mm (7.2 inches), thick.

1mm = 0.039 inches; 1 kPa = 0.145 psi; 1 kip = 4.45 kN

Details:

E = 27.56 GPa Poisson's ratio = 0.15
E_S = 52.9 MPa Poisson's ratio = 0.45
Slab : 4.57m x 4.57m

TABLE 2 Material and Geometric Properties of Flexible Pavement at Sherrard Section (*2*)

Layer	Material	Layer Thickness, mm	Young's Modulus, MPa	Poisson's Ratio	Density, kN/m^3
Surface	Asphalt Concrete	102	3445	0.35	22.7
Base	Crushed stone	356	241	0.40	22.0
Subgrade	A-4(6)	18288	69	0.45	18.0

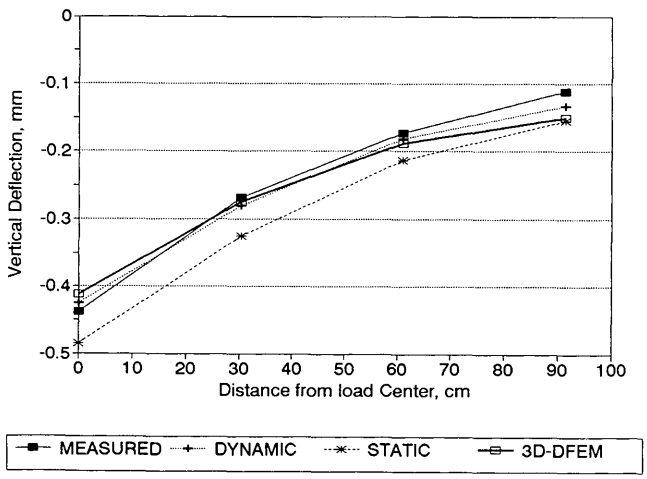

FIGURE 4 Measured, dynamic, static, and 3D-DFEM deflections at various distances for Sherrard section (1 mm = 39.37 mil; 1 cm = 0.393 in.).

STATISTICAL MODELS FOR DYNAMIC RESPONSE PREDICTION

Fractional Factorial Design

An experiment was designed to study the effect of layer thicknesses and moduli on pavement response. The following factors at various levels were considered in the factorial design:

- Surface layer (portland cement concrete) thickness (three levels),
- Base thickness (two levels),
- Subbase thickness (two levels),
- Concrete modulus (two levels),
- Base modulus (three levels),
- Subbase modulus (two levels),
- Subgrade modulus (three levels), and
- Pavement condition (three levels).

Table 3 gives the thickness and pavement moduli that were adopted for this study. The values are based on engineering judg-

TABLE 3 Attribute Values Used in Factorial Design

Factor	Number of levels		
	Level 1	Level 2	Level 3
Modulus of Surface layer, GPa (ksi)	20.7 (3000)	41.1 (6000)	-*
Modulus of base layer, GPa (ksi)	0.1 (15)	1.7 (250)	13.8 (2000)
Modulus of subbase layer, MPa (ksi)	69 (10)	170.0 (25)	-
Modulus of subgrade, MPa (ksi)	21 (3)	103 (15)	310 (45)
Thickness of surface layer, mm (in.)	203 (8)	254 (10)	330 (13)
Thickness of base layer, mm (in.)	102 (4)	203 (8)	-
Thickness of subbase layer, mm (in.)	0 (no subbase)	23 (8)	-

*Data not applicable

ment and experience. The number of levels attributed to each factor represents its full range of practical applications. To be of general use, different pavement condition scenarios need to be investigated, for example, both pavements in good condition with no discontinuity and, the other extreme, pavement in which the transverse joints have failed, resulting in voids at the joint. However, the present study concerns the first level only, that is, pavement in good condition.

Combinatorial design procedures were employed to assemble the experiment. A total of 1,296 combinations ($2^4 3^4$) were possible. Because it is prohibitively expensive to perform so many computational runs, a fractional factorial was adopted after Connor and Young (*15*). A one-eighth fraction replicate of the full factorial was selected for the study. For each combination, a response solution was obtained using 3D-DFEM, with the boundary conditions, material characterization, and FWD loading described earlier. The computations were performed on a Cray X-MP/16 supercomputer, and the desired responses (deflection, for instance) from each combination were stored in a data base for subsequent analysis.

Models for Deflection

Using the deflection data base, stepwise regression analyses were carried out developing statistical models for surface deflections at each geophone location of the FWD test setup. A SAS program was used for the analysis. For routine testing, many agencies, including SHRP, employ seven geophones, one at the center of the load and the remaining six at offset distances of 203, 305, 457, 610, 915, and 1,524 mm (8, 12, 18, 24, 36, and 60 in.), respectively. Two sets of seven model equations, one set for three-layer pavements and the other for four-layer pavements, are presented in Equations 1–14. The corresponding coefficients and R^2 values are listed in Table 4.

Equations for three-layer pavements:

$$D1 = A + B*\log_{10}E_4 + C*T_1 + D*T_2 + E*\log_{10}E_1*T_1 + F*\log_{10}E_2*T_2 \quad (1)$$

$$D2 = A + B*\log_{10}E_4 + C*T_1 + D*T_2 + E*\log_{10}E_1*T_1 + F*\log_{10}E_2*T_2 \quad (2)$$

$$D3 = A + B*\log_{10}E_4 + C*T_1 + E*\log_{10}E_1*T_1 + F*\log_{10}E_2*T_2 + G*\log_{10}E_1*\log_{10}E_2 + H*\log_{10}E_2*\log_{10}E_4 \quad (3)$$

$$D4 = A + B*\log_{10}E_4 + C*T_1 + E*\log_{10}E_1*T_1 + F*\log_{10}E_2*T_2 + G*\log_{10}E_1*\log_{10}E_2 + H*\log_{10}E_2*\log_{10}E_4 \quad (4)$$

$$D5 = A + B*\log_{10}E_4 + C*T_1 + E*\log_{10}E_1*T_1 + F*\log_{10}E_2*T_2 + G*\log_{10}E_1*\log_{10}E_2 + H*\log_{10}E_2*\log_{10}E_4 \quad (5)$$

$$D6 = A + B*\log_{10}E_4 + C*T_1 + E*\log_{10}E_1*T_1 + F*\log_{10}E_2*T_2 + G*\log_{10}E_1*\log_{10}E_2 + H*\log_{10}E_2*\log_{10}E_4 \quad (6)$$

$$D7 = A + B*\log_{10}E_4 + C*T_1 + D*T_2 + E*\log_{10}E_1*T_1 + F*\log_{10}E_2*T_2 + G*\log_{10}E_1*\log_{10}E_2 + H*\log_{10}E_2*\log_{10}E_4 \quad (7)$$

Equations for four-layer pavements:

$$D1 = A + B*\log_{10}E_1 + C*\log_{10}E_2 + D*\log_{10}E_4 + E*\log_{10}E_1*T_1 + F*\log_{10}E_2*T_2 + G*\log_{10}E_3*T_3 \quad (8)$$

$$D2 = A + B*\log_{10}E_1 + C*\log_{10}E_2 + D*\log_{10}E_4 + E*\log_{10}E_1*T_1 + F*\log_{10}E_2*T_2 + G*\log_{10}E_3*T_3 \quad (9)$$

TABLE 4 Summary of Regression Models for Three- and Four-Layer Pavements

Equation*	A	B	C	D	E	F	G	H	R^2-Value
1	8.6370	-2.1927	0.5499	0.1546	-0.2105	-0.0861	-**	-	0.9574
2	8.3554	-2.2848	0.4652	0.1433	-0.1824	-0.0785	-	-	0.9601
3	9.6629	-2.8505	0.3645	-	-0.1530	-0.0210	-0.1588	0.2175	0.9618
4	9.1665	-2.9167	0.3331	-	-0.1369	-0.0180	-0.1543	0.2401	0.9683
5	8.6785	-2.9514	0.3070	-	-0.1235	-0.0166	-0.1446	0.2546	0.9733
6	7.8922	-3.0162	0.2526	-	-0.1017	-0.0136	-0.1236	0.2477	0.9722
7	6.5106	-2.8653	0.1540	-0.0243	-0.0612	-	-0.1062	0.2072	0.9851
8	16.5614	-1.8386	-0.4273	-1.9043	-0.0563	-0.0321	-0.0769	-	0.9374
9	15.7317	-1.7182	-0.4303	-2.0004	-0.0452	-0.0279	-0.0944	-	0.9518
10	14.1212	-1.3992	-0.3976	-1.9930	-0.0424	-0.0244	-0.0859	-	0.9571
11	13.0566	-1.2514	-0.3704	-2.0168	-0.0351	-0.0197	-0.0893	-	0.9625
12	11.8815	-1.0759	-0.3394	-2.0295	-0.0284	-0.0151	-0.0920	-	0.9684
13	9.7651	-0.7922	-0.3242	-1.9254	-0.0180	-	-0.0944	-	0.9719
14	6.3211	-0.3994	-0.1686	-1.6979	-0.0054	-	-	-0.4973	0.9801

*Equations 1 through 7 are for three layered pavement systems and equations 8 through 14 are for four layered pavement systems.

**Data not applicable

$$D3 = A + B*\log_{10}E_1 + C*\log_{10}E_2 + D*\log_{10}E_4 + E*\log_{10}E_1*T_1 + F*\log_{10}E_2*T_2 + G*\log_{10}E_3*T_3 \quad (10)$$

$$D4 = A + B*\log_{10}E_1 + C*\log_{10}E_2 + D*\log_{10}E_4 + E*\log_{10}E_1*T_1 + F*\log_{10}E_2*T_2 + G*\log_{10}E_3*T_3 \quad (11)$$

$$D5 = A + B*\log_{10}E_1 + C*\log_{10}E_2 + D*\log_{10}E_4 + E*\log_{10}E_1*T_1 + F*\log_{10}E_2*T_2 + G*\log_{10}E_3*T_3 \quad (12)$$

$$D6 = A + B*\log_{10}E_1 + C*\log_{10}E_2 + D*\log_{10}E_4 + E*\log_{10}E_1*T_1 + G*\log_{10}E_3*T_3 \quad (13)$$

$$D7 = A + B*\log_{10}E_1 + C*\log_{10}E_2 + D*\log_{10}E_4 + E*\log_{10}E_1*T_1 + H*\log_{10}E_3 \quad (14)$$

where

$D_1, D_2, ..., D_7$ = sensor deflections 1, 2, ..., 7, respectively (mil);
E_i = modulus of ith layer (ksi), counting from surface to subgrade;
i = 1, 2, 3, 4;
T_i = thickness of ith layer (in.); and
$A, ..., H$ = regression coefficients (Table 4).

Note that the significance of the regression coefficients is evaluated using the respective t-ratios, a standard output of the SAS program. If the absolute value of the t-ratio is 2.0 or greater, the coefficient is considered reliable. On this basis, the coefficients of Equations 1–14 are highly significant. As can be noted from Table 4, the R^2 values range from 0.93 to 0.98 and are considered satisfactory.

In order to further confirm the robustness of the equations, standardized residuals are plotted against the predicted values to see whether they are distributed randomly. All 14 of the plots exhibited a random pattern, indicating the models' adequacy.

The sensitivity of the parameters was judged by the t-ratio, the premise being that the higher the t-ratio the greater the influence of that factor in the given relationship. As expected, the subgrade modulus influences the sixth and seventh sensor deflections significantly. For the other five sensor locations, again, subgrade modulus has the most influence on surface deflection.

Verification of Deflection Models

Models can be validated by comparing predicted and measured responses. Selected for comparison are three rigid pavement GPS sections of SHRP-LTPP from Mississippi. Table 5 indicates the layer thickness and elastic properties of two of these sections: one three-layer section and one four-layer section. The concrete moduli and the FWD deflection data were assembled from the SHRP data base, whereas the subgrade moduli were furnished by the SHRP regional contractor through the research division at the Mississippi DOT. For want of accurate information, the base and subbase moduli were estimated on the basis of laboratory results (*16*). Adopting these properties and inputting them into Equations 1–7 for three-layer sections and into Equations 7–14 for four-layer sections, the authors calculated seven sensor deflections for the two cases. In Figure 5, the predicted deflection basin is compared with the measured FWD basin for three-layer pavement. Also

TABLE 5 Layer Thicknesses and Properties of SHRP Sections Used for Comparisons of Deflection Bowls

Layer Properties	Three Layer Section (SHRP Sec. No 285803)	Four Layer Section (SHRP Sec. No. 285805)
Thickness of Surface Layer, mm (in.)	203 (8)	203 (8)
Thickness of Base Layer, mm (in.)	152 (6)	102 (4)
Thickness of Subbase Layer, mm (in.)	-*	178 (7)
Modulus of Surface Layer, GPa (ksi)	32.1 (4650)	39.0 (5650)
Modulus of Base Layer, GPa (ksi)	11.7 (1700)	3.5 (500)
Modulus of Subbase Layer, MPa (ksi)	-	137.6 (20)
Modulus of Subgrade, MPa (ksi)	81.7 (11.87)	75.6 (10.99)

*Data not applicable

plotted are deflection basins from direct solution of the 3D-DFEM and the multilayered elastic program BISAR. The predictions for the first five sensor locations are within ±5 percent of the field deflections, whereas the sixth and seventh sensors differ from the field deflections by 17 and 36 percentage points, respectively. Similar comparison of a four-layer system (Figure 6) indicates that predicted deflections consistently are larger than the measured ones, the average error being less than 15 percent. One factor contributing to this discrepancy may be the one-eighth factorial selected for the study; it may be insufficient to account for all interactive effects that arise in the model. Other reasons for the discrepancy may include the need for realistic (viscoelastic) characterization of subgrade and base layers, and the approximate moduli adopted for base and subbase. Static analysis, in both cases, overpredicts the field deflections by as much as 80 percent, however. Due in part to the discrepancy between dynamic and static deflections, the traditional backcalculation procedures, (in which the objective is to match the dynamic load basins with static deflections) would in all likelihood overpredict the layer moduli. This strongly suggests the need for employing dynamic load representation for pavement analysis or response equations—a much needed revision in backcalculation routines.

SUMMARY AND CONCLUSIONS

To improve on the current pavement analysis procedure, a 3D-DFEM was formalized. The 3D-DFEM can simulate moving or impulse loads and linear and nonlinear material properties. Response analysis with various boundary conditions and element aspect ratios helped to finalize an appropriate model geometry that was later used to model rigid pavements. An investigation was conducted with 3D-DFEM, establishing the model's validity in solving static and, more importantly, dynamic problems.

A one-eighth fractional factorial experiment was designed on the basis of pavement response to FWD loading (deflection, for instance) as a function of pavement geometry and material characteristics. Statistically significant equations were developed and the data base generated from computer models of 54 different combinations. The equations, in turn, were validated by predicting the measured deflections of two in-service rigid pavements. The average error resulting at each sensor location from the predictions was less than 15 percent. Significant to note, however, was that static deflections were larger than their dynamic counterparts. Larger apparent deflection response could result in overprediction

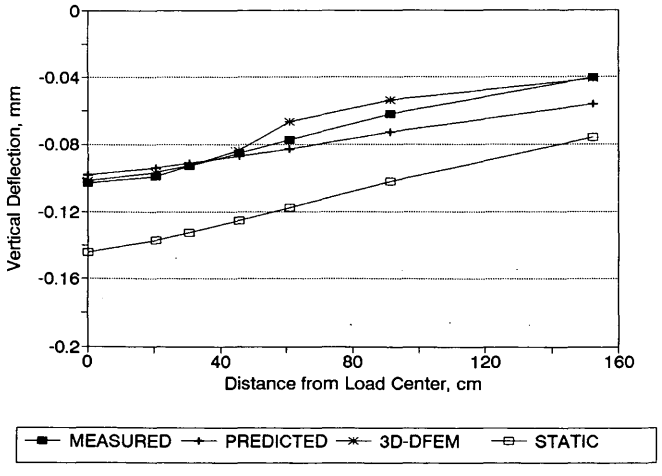

FIGURE 5 Measured, predicted, 3D-DFEM, and static deflections at various distances for SHRP Section 285803, SHRP FWD Test No. 300267 (1 mm = 39.37 mil; 1 cm = 0.393 in.).

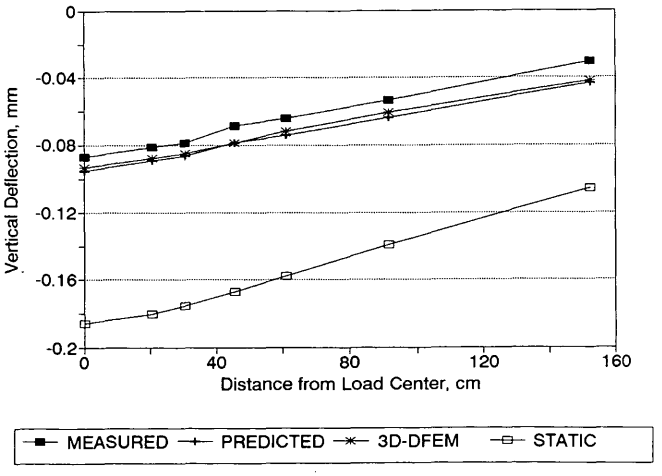

FIGURE 6 Measured, predicted, 3D-DFEM, and static deflections at various distances for SHRP Sec. 285805, SHRP FWD Test No. 300151 (1 mm = 39.37 mil; 1 cm = 0.393 in.).

of layer moduli in backcalculation algorithms. In short, static response analysis, traditionally employed in backcalculation algorithms, should be replaced with dynamic analysis routines. The 3D-DFEM program, with its numerous features simulating real-world pavement loading, is a needed tool for analyzing the response of flexible- and rigid-pavement structures.

ACKNOWLEDGMENTS

Alfred Crawley of the Mississippi DOT told the authors of a preliminary study to model a rigid pavement in Mississippi that had sustained premature cracking. Waheed Uddin and Robert Hackett of the Department of Civil Engineering, University of Mississippi, contributed immensely to adapting ABAQUS for rigid pavement analysis. The study was supported in part by the Department of Civil Engineering, in cooperation with the Office of Computing and Information Systems, of the university.

REFERENCES

1. Mamlouk, M. S. Use of Dynamic Analysis in Predicting Field Multilayer Pavement Moduli. In *Transportation Research Record 1043*, TRB, National Research Council, Washington, D.C., 1985, pp. 113–121.
2. Sebaaly, B. E., M. S. Mamlouk, and T. G. Davies. Dynamic Analysis of Falling Weight Deflectometer Data. In *Transportation Research Record 1070*, TRB, National Research Council, Washington, D.C., 1986, pp. 63–68.
3. Ashton, J. E., and F. Moavenzadeh. The Analysis of Stresses and Displacements in a Three-Layered Viscoelastic System. *Proc., International Conference, Structural Design of Asphalt Pavements*, 1967.
4. Ioannides, A. M. Finite Difference Solution for Plate on Elastic Solid. *Journal of Transportation Engineering*, Vol. 114, No. 1, ASCE, New York, Jan. 1988, pp. 57–75.
5. Ioannides, A. M. *Analysis of Slabs-on-Grade for a Variety of Loading and Support Conditions*. Report TR-85-0083. U.S. Air Force Office of Scientific Research, Air Force Systems Command, U.S. Air Force, Washington, D.C., Sept. 1984.
6. Ioannides, A. M., M. R. Thompson, and E. J. Barenberg. Finite Element Analysis of Slabs-on-Grade Using a Variety of Support Models. *Proc., Third International Conference on Concrete Pavement Design and Rehabilitation*, Purdue University, West Lafayette, Ind., April 1985, pp. 309–324.
7. Ioannides, A. M., and J. P. Donnelley. Three-Dimensional Analysis of Slab on Stress-Dependent Foundation. In *Transportation Research Record 1196*, TRB, National Research Council, Washington, D.C., 1988.
8. *ABAQUS, Finite Element Computer Program*. Hibbit, Karlsson, Sorenson, Inc., 1989.
9. Zaghlou, S., and T. D. White. Use of a Three-Dimensional-Dynamic Finite Element Program for Analysis of Flexible Pavement. In *Transportation Research Record No. 1388*, TRB, National Research Council, Washington, D.C., 1993, pp. 60–69.
10. Zaghloul, S., T. D. White, V. P. Drnevich, and B. Coree. Dynamic Analysis of FWD Loading and Pavement Response Using a Three-Dimensional Dynamic Finite Element Program. In *Nondestructive Testing of Pavements and Backcalculation of Moduli*, Vol. 2. STP 1198, ASTM, Philadelphia, Pa., 1994.
11. Bohn, A., P. Ullidtz, R. Stubstad, and A. Sorensen. Danish Experiments with the French Falling Weight Deflectometer. *Proc., 3rd International Conference on the Structural Design of Asphalt Pavements*, London, England, Sept. 11–15, 1972, pp. 1119–1128.
12. Losberg, A. *Structurally Reinforced Concrete Pavements*. Doktrsavhandlingar Vid Chalmers Tekniska Hogskola, Göteborg, Sweden, 1960.
13. *Bitumen Structures Analysis In Roads (BISAR) Computer Program*. Koninlilijke/Shell-Laboratorium, Amsterdam, Netherlands, July 1972.
14. Hoffman, M. S., and M. R. Thompson. *Nondestructive Testing of Flexible Pavements: Field Testing Program Summary*. Transportation Engineering Series 31, Illinois Cooperative Highway and Transportation Research Program, Series 188. University of Illinois at Urbana Champaign, Urbana, June 1981.
15. Connor, W. S., and S. Young. *Fractional Factorial Designs for Experiments with Factors at Two and Three Levels*. National Bureau of Standards, Applied Mathematics Series-58. Sept. 1961.
16. George, K. P. *Material Parameters for Pavement Design Using AASHTO Interim Guide*. Final Report. Department of Civil Engineering, University of Mississippi, University, 1981.

The opinions, findings, and conclusions expressed in this report are those of the authors and not necessarily those of the sponsoring organizations.

Publication of this paper sponsored by Committee on Modeling Techniques in Geomechanics.